Chemistry and Materials Research
ISSN 2224- 3224 (Print) ISSN 2225- 0956 (Online)
Vol.6 No.6, 2014

Post-fabrication annealing effects on the performance of polymer: Fullerene solar cells with ZnO nanoparticles

Mohammed K. Hamad[1]. , Hussein F. Al-luaiby[2] Waleed A. Hussain [2] and Assel K. Hassan[3]
1. Department of physics, college of education, Basrah University
2. Department of physics, college of education, Basrah University
3. Materials and Engineering Research Institute, Sheffield Hallam University

* E-mail of the corresponding author: mohammed.kazum@yahoo.com

Abstract

In this study, poly(3-hexylthiophene):[6,6]-phenyl C61-butyric acid methylester (P3HT:PCBM) organic photovoltaic (OPV) devices, with ZnO nanoparticles buffer layer between the photoactive layer (P3HT:PCBM) and the cathode (Al top electrode), were fabricated. The active layer were annealed at 140 ^{o}C before depositing the Zno and top electrode. The objective of this study was to investigate the effects of the ZnO buffer layer and pre-/post-fabrication annealing on the general performance of these devices. The short-circuit current density(J_{SC}) and open-circuit voltage (V_{OC}) of the OPV devices were improved by the insertion of the ZnO layer and post-fabrication annealing. This can be attributed to, among other things, improved charge transport across the interface between the photoactive layer and the Al top electrode as a result of post-annealing induced modification of the interface morphology.

Keywords: Organic, Photovoltaic, Heterojunction, Carriers.

1. Introduction

Since the discovery of their electroluminescence [1], conjugated polymers have been extensively studied for a wide range of optoelectronic applications such as polymer light emitting diodes [2] and organic photovoltaic devices [3]. The advantage of conjugated polymers over other electronic materials is that they can be readily processed into thin films from solution using techniques such as spin coating or inkjet printing [4], thereby offering the prospect of low cost manufacturing processes. However, the morphology of a bulk-heterojunction, consisting of a binary blend, cannot be easily controlled. The formation of the final blended structure is affected by several parameters, such as the blend composition, viscosity, solvent evaporation rate [5] and substrate surface energy, all of which present difficulties in the achievement of the desired blend morphology for maximum charge generation and transport [6].
nowadays, organic solar cell/photovoltaic (OPV) devices, fabricated from th blends of poly(3-hexylthiopene)(P3HT) and ([6,6]-phenyl C61-butyric acid methylester)(PCBM), are the most widely studied bulk heterojunction systems because of their relatively good photovoltaic (PV) properties. Although the P3HT:PCBM devices exhibit excellent PV properties compared to other bulk heterojunction OPV devices[7], their power conversion efficiency (PCE) is still too low compared to that of the conventional silicon PV cells. As discussed in other papers [8–9], the space charge buildup caused by a low mobility of charge carriers is one of the factors that limits the (PCE) and/or the fill factor (FF) by lowering the open-circuit voltage (V_{OC}) and short-circuit current density (J_{SC}) of the devices. Furthermore, Al atoms from the top electrode may diffuse into the photoactive layer during the ageing of the devices and act as quenching/recombination centers while the penetration of water and/or oxygen molecules through the top electrode via pin hole and grain boundaries during operation or storage in air may lead to photo-oxidation and degradation of the devices [10-11]. One way of improving the performance of the P3HT:PCBM devices is to insert a metal oxide buffer layer between the photoactive layer (P3HT:PCBM) and the cathode (Al top electrode). For example, an improved performance was observed when ZnO [10,12] and TiO2 [13] nanoparticles were used as buffer layers between the active layer and the cathode.Qian etal. [10] speculated that, the ZnO layer prevents diffusion of Al atoms into the active layer and also has the potential to improve the environmental stability of the OPV devices by absorbing UV photons that could lead to bond breaking or photo-oxidation in the presence of water and/or oxygen molecules. They demonstrated an improved stability and a 30–80% improvement in (PCE) of PH3T:PCBM OPV devices with the ZnO buffer layer. In addition, post-fabrication annealing is also known to improve the (PCE) of OPV devices. For example, Mihailetchi [8] demonstrated a tenfold increase in (PCE) from post-fabrication annealed P3HT:PCBM devices (any metal oxide buffer layer) compared to similar devices that were not annealed. They attributed the increasing to enhanced hole mobility in the P3HT phase. In this study, P3HT:PCBM devices with the ZnO layer, were fabricated and they were annealed before depositing the Al metal top electrode. This paper sets out to discuss the combined effects of the ZnO buffer layer and pre-/post-fabrication annealing on the general performance of the P3HT:PCBM devices.

2. Experiment

2.1. Materials and chemicals

The water solution of poly (3,4ethylenedioxythiophene):poly(styrenesulfonate) (PEDOT:PSS) layer (from

Sigma-Aldrich) which acted as the anode buffer layer to modify the work function of indium tin oxide (ITO) on glasses (80 nm in thickness and 25 Ω/sq sheet resistance) and as the hole transport layer (hTL) on ITO bottom electrode. The chlorobenzene solution of poly (3- hexylthiophene) (P3HT) from Aldrich and [6,6]-phenyl C61-butyric acid methylester (PCBM) from Aldrich with a mixture ratio of 1:1 was made to produce the active layer for light absorption. The ZnO sol was prepared by dissolving 0.1 M zinc acetate dehydrate (from Aldrich) in 2-methoxyethanol and then ethanolamine was added as the stabilising agent. The molar ratio of zinc acetate to ethanolamine is at 1:1. The prepared ZnO sol was used to produce an amorphous ZnO layer which used as received for fabrication of the electron transport layer.

2.2. characterization

Current–voltage characteristics of OPV devices were conducted on the computer controlled Kithely sourcemeter. Illumination was provided by a solar simulator with AM1.5G spectra at 100 mW/cm2. The UV-vis absorption spectra of the polymer films were recorded on Varian 50 scan UV-visible spectrophotometer. The blend structures were investigated by multipurpose X'Pert PHLIPS X-Ray defractometer (MPD), and the film thickness was determined using M2000V (J.A. Woollam Co., Inc.) spectroscopic ellipsometer, operating in the wavelength range 370-1000 nm. The scanning electron microscope (SEM) and the tapping mode atomic force microscope (AFM) images were recorded using FEI™ Nova Nano SEM and Vecco Nanoscope III AFM, respectively.

2.3. OPV device fabrication

Pre-structured ITO coated glass substrates (80 nm in thickness and 25 Ω/sq sheet resistance) were ultrasonically cleaned in acetone, isopropyl alcohol and deionised water for 10 min, respectively. After drying with nitrogen, the substrates were spin-coated with a ~25 nm thin PEDOT:PSS layer and then transferred again into the nitrogen-filled glovebox for heat annealed at 110 ^{o}C for 10 min. On top of the PEDOT:PSS layer, a ~160 nm thick active layer was spin-coated from the chlorobenzene solution of P3HT:PCBM and then was annealed at 140 ^{o}C for 10 min on a hot plate. Afterwards, the samples were removed out of the glovebox, followed a _40 nm thin amorphous ZnO layer by the sol–gel method and spin coating deposited then annealed on a hot plate at 150 ^{o}C for 10 min. Then the samples were transferred into a nitrogen-filled glovebox. Finally, a electrode consisting of 100 nm Al was thermally evaporated under vacuum of ~ 1×10-5 torr with a rate of deposition of 0.2 nm/s onto the Zno layer surface. The active layer were subjected to a thermal annealing process (80–140 °C) for 10 min . The electrode was already deposited onto the ZnO layer prior to all annealing processes. The schematic diagram of ITO\ PEDOT:PSS\P3HT:PCBM\ ZnO\ Al device processing structures is shown in Fig. 1a

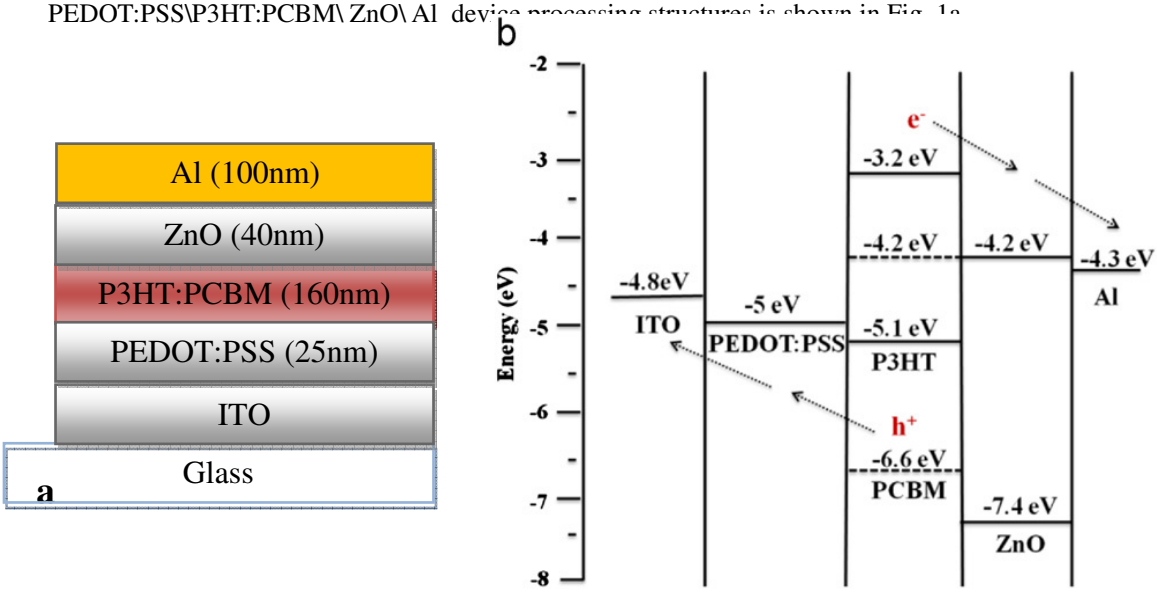

Fig. 1. (a) Device structure of the organic solar cell with the electron extraction layer of ZnO nanostructures and (b) the energy level diagram of each component of the device (the energies are referenced to the vacuum level) .

3. Results and discussion

The sol-gel technique is a convenient method for fabrication of OPV devices and demands only solution based deposition methods using low process temperature, which guarantees low cost and large-scale production. Fig. 2a shows the SEM image of the sol–gel derived ZnO thin film on ITO coated glasses. It presented amorphous structures. The AFM image in Fig. 2b shown its mean roughness below 4 nm and it covered the whole surfaces of

the ITO thin films [14]. The AFM morphology of P3HT:PCBM blends is showed in Fig. 3 and this phenomenon accords with the change of root means square (RMS) roughness of the active layer from 0.331 to 1.984 nm before and after annealing, which was calculated according to the AFM images [15]. It has been considered that a larger RMS is a 'signature' of high-efficiency solar cells in 'thermal annealing' [16]. Fig.3 shows the surface morphology of P3HT:PCBM before and after annealing measured by AFM. It is apparent that the surface roughness of P3HT:PCBM was increased due to the vertical phase separation during annealing, the $PC_{60}BM$ molecular could easily penetrate into the bulk of active layer and left some hollows on the film surface during annealing [15] .In Fig.3, we observe that highly improved RMS occurs at 140 ^{o}C, which might illuminate that higher performances are achieved after 140 ^{o}C annealing. With additional annealing, the RMS increases.

The optical absorption spectra of PCBM and P3HT thin films were recorded before and after the annealing at 140 ^{o}C (Fig.4(a) and (b)). The P3HT thin films showed a slight increase in the absorption band at 445 – 640 nm after annealing, which concurs with the literature [17]. An increase in the absorption band after annealing generally indicates increased packing of the P3HT domains [18]. The absorption peak moved towards longer wavelengths with increasing temperature because polymers with shorter conjugation lengths can absorb higher energy photons [17]. The PCBM thin films (Fig. 4(a)) showed no significant change in the optical absorption behavior when the annealing temperature was varied.

Therefore, the changes in the PCBM/P3HT thin films were attributed to the changes in the polymer, P3HT. Figure 4(c) presents the absorption spectra of the annealed PCBM/ P3HT composite films at different temperatures (RT,80,120,140) ^{o}C. The untreated film (at room temperature ~30 ^{o}C) showed a dominant broad absorption peak at approximately 445 – 640 nm and a relatively weak shoulder peak at approximately 530 nm and 580 nm. The absorption spectra of the blend films were combinations of two spectra, one from PCBM and the other from P3HT. The intensity of the absorption peak at approximately 445 – 640 nm increased and moved to longer wavelengths as the thermal annealing temperature was increased from room temperature to 140 ^{o}C . On the other hand, the intensity of the absorption peak decreased after annealing at temperature higher than 140 ^{o}C, indicating that the inter-diffusion between the PCBM and the P3HT components started to occur.

The annealing has an important impact on the crystallinity of P3HT. We can observe the increased crystallinity of P3HT in XRD results as shown in Fig.5. Compared with room temperature annealing, the crystallinity is increased in the peak at 2θ=5.4° after to 140 ^{o}C annealing [19]. The conjugated chain is fully self-assembled to be orderly structure, the length of conjugated bond is increased, and the increased thermal diffusion of PCBM molecules at elevated temperatures into larger PCBM aggregates [20,21,22]. As a result of this motion, the regions with low PCBM concentration occur. In these PCBM free regions, the P3HT aggregates can become converted into P3HT crystallites [23]. Note that the P3HT crystallinity is the highest for the annealing temperature of 140 ^{o}C. Further increase of the annealing temperature leads to a decrease of the P3HT crystallinity. We presume that the P3HT crystallites become unstable due to enhanced thermal motion of the P3HT molecules at high temperatures, which results in ''melting'' of P3HT crystallites and thus in a reduction of the P3HT crystallinity [20].

The current density–voltage (J–V) characteristics of the ZnO/P3HT:PCBM devices with annealed at different temperatures, are shown in Fig.6 and Table 1. The photovoltaic properties were studied under AM 1.5 G conditions with a light intensity of 100 mW/cm^2. The current density–voltage (J–V) characteristics are listed in Table 1. It is evident from Fig. 6a and Table 1 that the device based on the ZnO/P3HT:PCBM/PEDT structure exhibits an improved short-circuit current density (Jsc) and fill factor (FF), as well as a higher power conversion efficiency (PCE) of approximately 3.8%. The statistical data for the annealed devices are shown in Fig. 7. After annealing at 80 °C, the Jsc and FF increased, resulting in an estimated PCE of 1.6%. A further increase in annealing temperature to 140 °C (Fig. 7a) induced a remarkable increase in the Jsc, FF and PCE values. This result was attributed to the improved absorption of the incident light and the charge transportation properties of the highly ordered P3HT crystallites [24]. Motaung [25] and [26,27] showed that the PCEs of solar cells improve upon placing the cells in air for a few days due to the self-organisation of the P3HT/PCBM layer and oxidation of the silver electrode with time, resulting in a significant enhancement of the Jsc, FF and open circuit voltage (Voc). However, a decline in the Voc was observed with the annealing temperature, as shown in Fig. 7b. Guo et al. [27] reported that a decrease in the open circuit voltage may be due to a reduction in the work function of the Pt electrodes or due to the formation of shunts. When the annealing temperature increased to 160 ^{o}C, the devices degraded, as depicted in the photovoltaic performances shown in Fig. 7.

4. Conclusion

We have investigated the combined effects of the post-fabrication annealing and ZnO buffer layer on the general performance of the P3HT:PCMB based OPV devices. An improvement in photovoltaic properties was observed from the devices annealed before depositing the Al top electrode compared to similar devices annealed at room temperature. While we expect the post-annealed device with the ZnO layer to exhibit improved PV properties, the greatest improvement was observed from the post annealed device with the ZnO layer and the possible

mechanism for this improvement was discussed.

References

J.H. Burroughes, D.D.C. Bradley, A.R. Brown, R.H. Marks, K. Mackay, R.H. Friend, P.L. Burn, A.B. Holmes, Nature 347 (1990) 539.
R.H. Friend, R.W. Gymer, A.B. Holmes, J.H. Burroughes, R.N. Marks, C. Taliani, D.D.C. Bradley, D.A. Dos Santos, J.L. Brédas, M. Lögdlund, W.R. Salaneck, Nature 397 (1999) 121.
C.J. Brabec, V. Dyakonov, J. Parisi, N.S. Sariciftci, Organic Photovoltaics: Concepts and Realization, vol. 60, Springer, Berlin, 2003.
T.R. Hebner, C.C. Wu, D. Marcy, M.H. Lu, C. Sturm, Appl. Phys. Lett. 72 (1998) 519.
D.E. Motaung, G.F. Malgas, C.J. Arendse, Synth. Met. 160 (2010) 876.
M.N. Yusli, T. Way Yun, K. Sulaiman, Mater. Lett. 63 (2009) 2691.
Wei. Wei , Xin. Liu , Yanmin Wanga, YijieGu, Solar Energy Materials & Solar Cells. 98 (2012) 129–145
V.D. Mihailetchi, H. Xie, B. de Boer, L.J.A. Koster, P.W.M. Blom, Adv. Funct. Mater. 16 (2006) 699.
H. Kim, W.-W. So, S.-J. Moon, Sol. Energy Mater. Sol. Cells 91 (2007) 581.
L. Qian, J. Yang, R. Zhou, S. Tang, Y. Zheng, T.-K. Tseng, D. Bera, J. Xue, P.H. Holloway., J. Mater. Chem. 21 (2011) 3814.
O.M. Ntwaeaborwa a,n, RenjiaZhou b, LeiQian b, ShreyasS. Pitale a, J.Xue b, H.C.Swart a, P.H.Holloway b Physica B 407 (2012) 1631–1633
S.K. Hau, H.-L. Yip, N.S. Baek, J. Zou, K. O'Malley, A.K.-Y. Jen., Appl. Phys. Lett. 92 (2008) 253301.
K. Lee, J.Y. Kim, S.H. Park, S.H. Kim, S. Cho, A.J. Heeger., Adv. Mater. 19 (2007) 2445.
Ku. Vikas, Heming Wang Organic Electronics 14 (2013) 560–568
Xu. Xiaowei , Fu. Zhang , Jian Zhang Hui Wang , Zuliang Zhuo , Yang Liu , Jian Wang , Zixuan Wang , Zheng Xu, Materials Science and Engineering C 32 (2012) 685–691
X. Fan · G.J. Fang · P.L. Qin · F. Cheng · X.Z. Zhao Appl Phys A (2011) 105:1003–1009
O. Inganas, W. R. Salaneck, J. E. Osterholm and J. Laakso, Synth. Meter. **22**, 39 (1988).
H. Sirringhaus, P. J. Brown, R. H. Friend, M. M. Nielsen, K. Bechgarrd, B. M. W. Langeveld- Voss and D. M. de Leeuw, Nature **401**, 685 (1999).
YU Xuan, YU Xiao-ming , HU Zi-yang, ZHANG Jian-jun , ZHAO Gengshen and ZHAO Ying , Vol.9 No.4, 1 July 2013 .
Erb. Tobias, U.K Uladzimir Zhokhavets , Harald Hoppe, Gerhard Gobsch ,Maher Al-Ibrahim, Oliver Ambacher b Thin Solid Films 511 – 512 (2006) 483 – 485
H. Hoppe, M. Niggemann, C. Winder, J. Kraut, R. Hiesgen, A. Hinsch, D. Meissner, N.S. Sariciftci, Adv. Funct. Mater. 14 (2004) 1005.
X. Yang, J.K.J. van Duren, R.A.J. Janssen, M.A.J. Michels, J. Loos, Macromolecules 37 (2004) 2151.
T. Erb, U. Zhokhavets, G. Gobsch, S. Raleva, B. Stu¨ hn, P. Schilinsky, C. Waldauf, C. Brabec, Adv. Func. Mat. 15 (2005) 1193.
M.T. Khan, R. Bhargav, A. Kaur, S.K. Dhawan, S. Chand, Thin Solid Films 519 (2010) 1007.
M.-Y. Liu, C.-H. Chang, C.-H. Chang, K.-H. Tsai, J.-S. Huang, C.-Y. Chou, I.-J. Wang, P.-S.Wang, C.-Y. Lee, C.-H. Chao, C.-L. Yeh, C.-I. Wu, C.-F. Lin, Thin Solid Films 518 (2010) 4964.
Y. Guo, H. Geng, Thin Solid Films 519 (2011) 2349.
E. David. Motaung , F. Gerald. Malgas , Suprakas S. Ray , Christopher J. Arendse Thin Solid Films 537 (2013) 90–96.

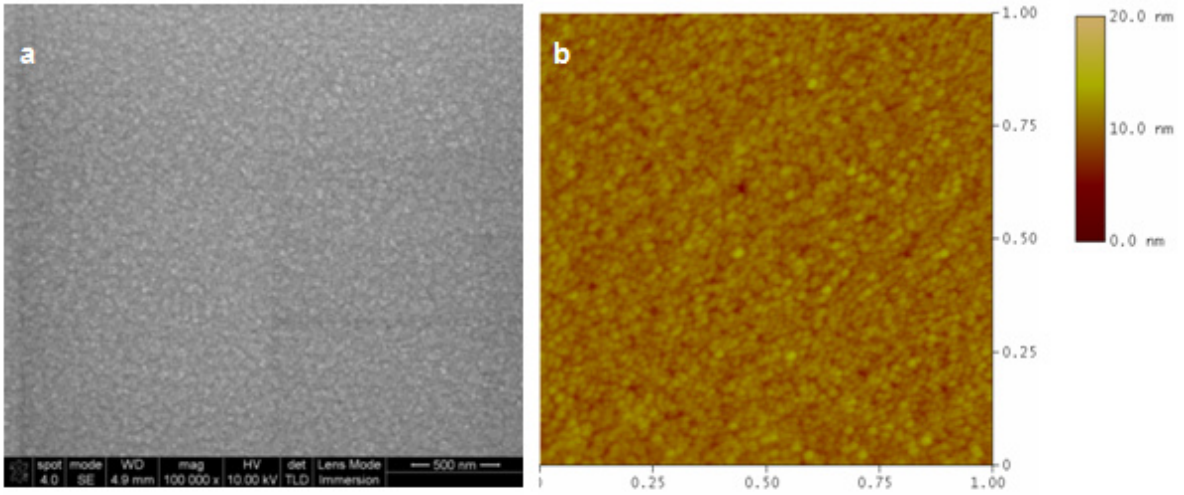

Fig. 2. Morphologies of sol–gel derived ZnO thin films on active layer; (a) SEM images presenting an amorphous structure and (b) AFM images indicating a very smooth surface.

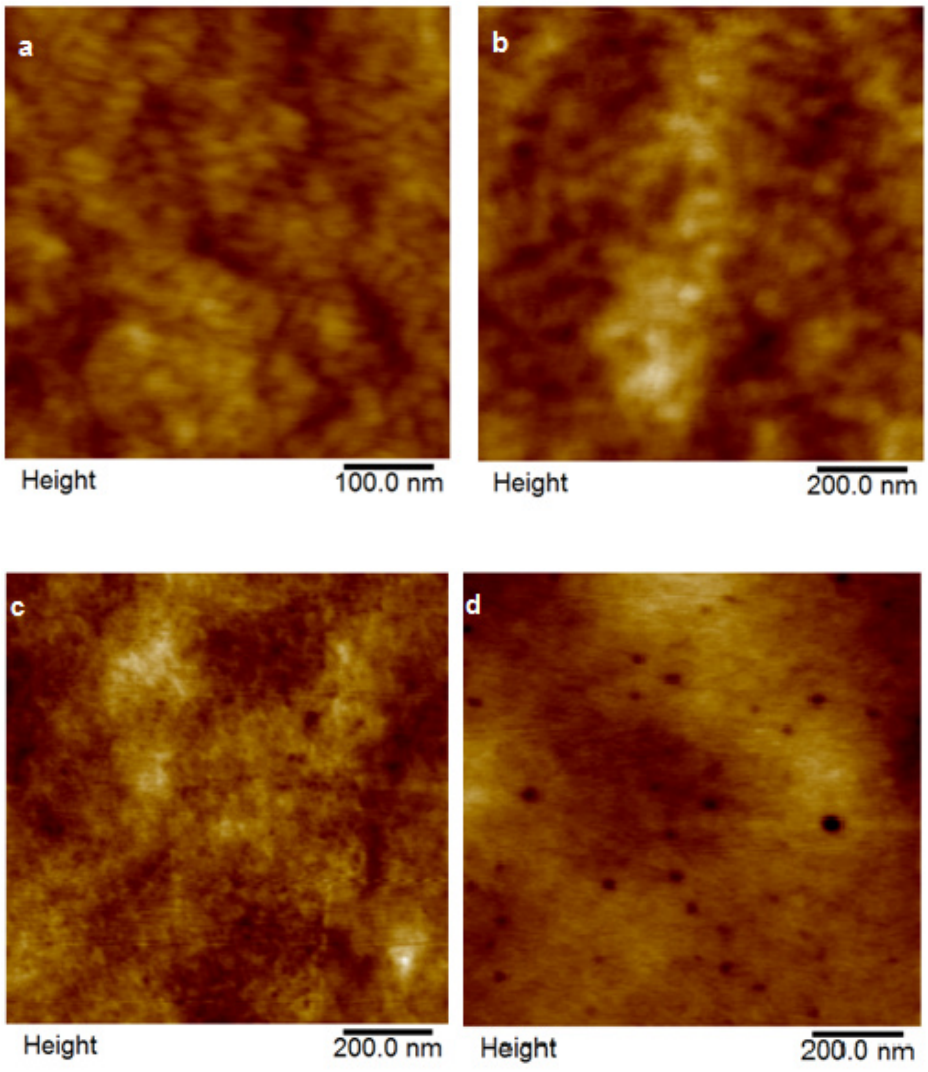

Fig. 3 AFM images of P3HT:PCBM films spin-coated from chlorobenzene with annealing at room

temperature (**a**) and annealed for 80C (**b**),120C (**c**), 140C (d)

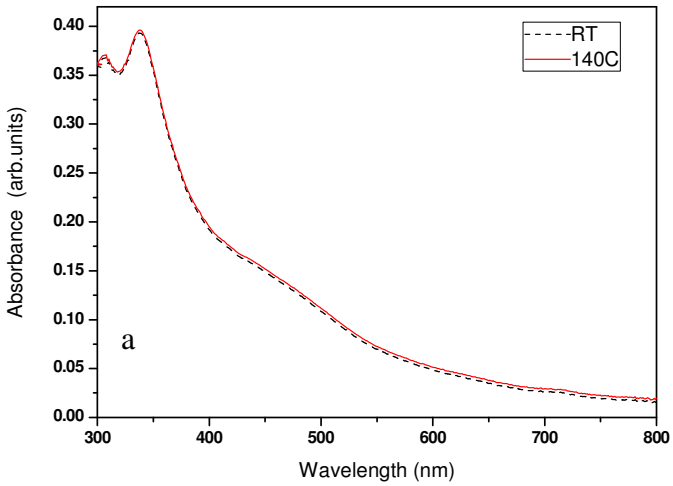

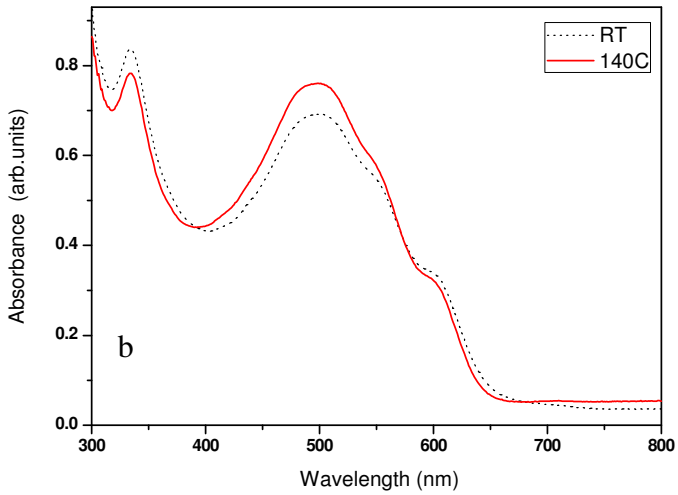

Fig. 4. (shown) UV-vis Absorption spectra of thin films of (a) PCBM and (b) a P3HT thin films, And (c) a P3HT/PCBM composite film

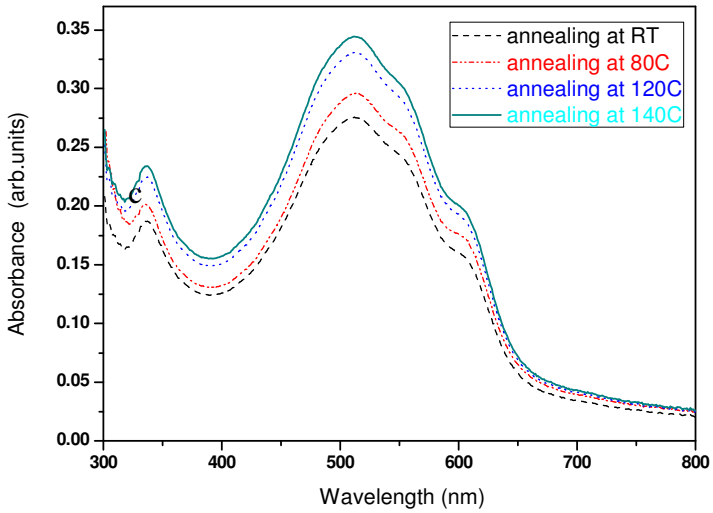

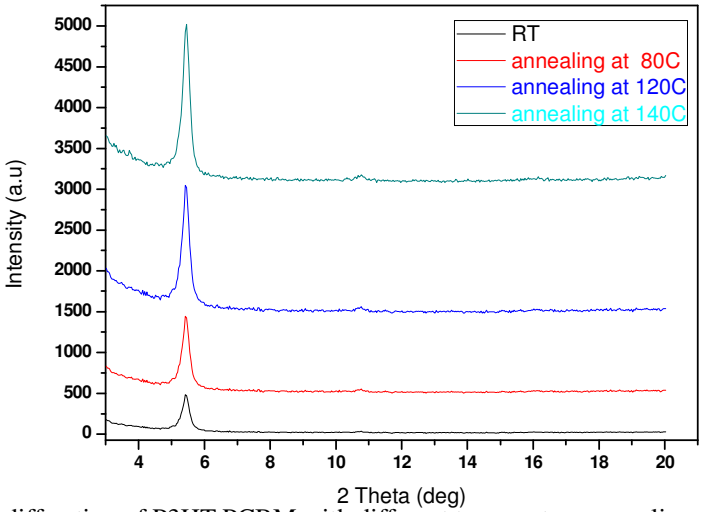

Fig. 5. X-ray diffraction of P3HT:PCBM with different temperature annealing treatment .

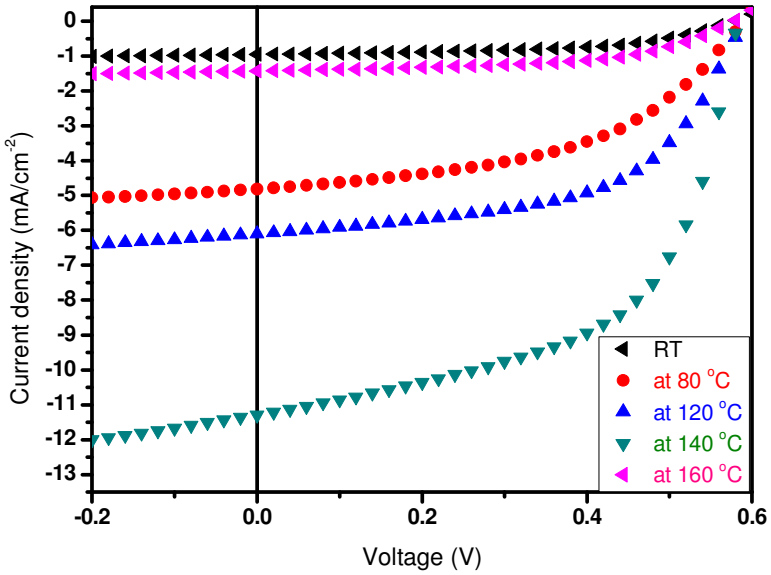

Fig. 6. Current density–voltage (J–V) characteristics of the (a) annealed ZnO/P3HT:PCBM at temperatures ranging from 80 to 140°C

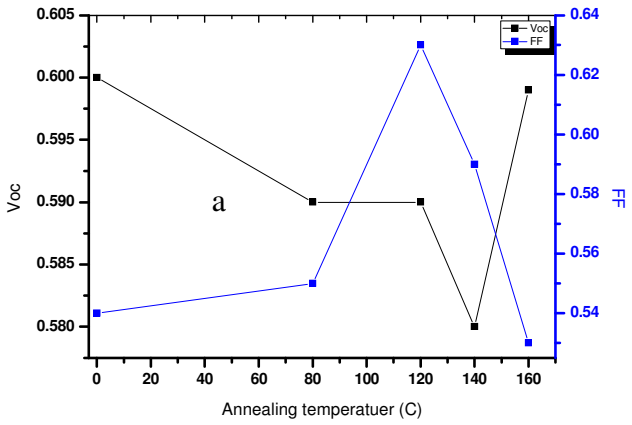

b

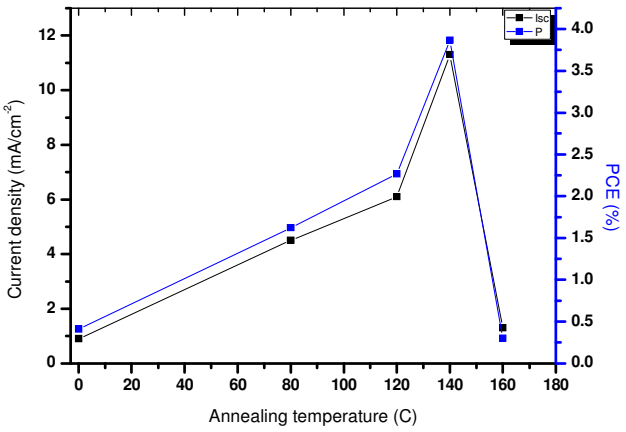

Fig. 7. Statistical data for the various annealed ZnO/P3HT:PCBM devices (a) Voc and FF and (b) Jsc and PCE. It should be noted that the films were annealed from 80 to 140 °C.

Table 1 Summary of performance for devices (ZnO/P3HT: PCBM (1:1)) .

Annealing	**Voc(v)**	**Jsc (mA/ cm^{-2})**	**FF**	**PCE(%)**
RT	0.6	0.95	0.54	0.3078
80 ^{o}C	0.59	5	0.55	1.6225
120 ^{o}C	0.59	6.1	0.63	2.2673
140 ^{o}C	0.58	11.3	0.59	3.8668
160 ^{o}C	0.56	1.1	0.53	0.3307

The IISTE is a pioneer in the Open-Access hosting service and academic event management. The aim of the firm is Accelerating Global Knowledge Sharing.

More information about the firm can be found on the homepage:
http://www.iiste.org

CALL FOR JOURNAL PAPERS

There are more than 30 peer-reviewed academic journals hosted under the hosting platform.

Prospective authors of journals can find the submission instruction on the following page: http://www.iiste.org/journals/ All the journals articles are available online to the readers all over the world without financial, legal, or technical barriers other than those inseparable from gaining access to the internet itself. Paper version of the journals is also available upon request of readers and authors.

MORE RESOURCES

Book publication information: http://www.iiste.org/book/

IISTE Knowledge Sharing Partners

EBSCO, Index Copernicus, Ulrich's Periodicals Directory, JournalTOCS, PKP Open Archives Harvester, Bielefeld Academic Search Engine, Elektronische Zeitschriftenbibliothek EZB, Open J-Gate, OCLC WorldCat, Universe Digtial Library , NewJour, Google Scholar